Electronic Supplementary Information

Macrocyclic tetranuclear Zn^{II} complex as receptor for selective dual fluorescence sensing of F^- and AcO^-: effect of macrocyclic ligand

Tonmoy Chakraborty,[a] Sanchari Dasgupta,[a] Arghyadeep Bhattacharyya,[a] Ennio Zangrando,[b] Daniel Escudero,*[,c] Debasis Das*[,a]

[a]Department of Chemistry, University of Calcutta, 92 A. P. C. Road, Kolkata 700009, India.
[b]Department of Chemical and Pharmaceutical Sciences, University of Trieste, Via L. Giorgieri 1, 34127 Trieste, Italy.
[c]Department of Chemistry, KU Leuven, Celestijnenlaan 200F, B-3001 Leuven, Belgium.

E-mail: *dasdebasis2001@yahoo.com*, *daniel.escudero@kuleuven.be*

Contents of the Supporting Information

medium at 25 °C.

Fig. S11 UV-Vis titration of **DAS** (25 μM) with F^-, inset shows calibration curve for determination of LOD.

Fig. S12 Job's plot for the determination of **DAS**-F^-/AcO^- (1:1) complex stoichiometry using absorbance values.

Fig. S13 UV-Vis titration of **DAS** (25 μM) with AcO^- in (a) methanol (b) acetonitrile (c) acetonitrile-methanol (2:1) medium at 25 °C.

Fig. S14 Fluorescence spectrum of **DAS** (25 μM) in presence of all anions (F^-, AcO^-, Cl^-, I^-, S^{2-}, PO_4^{3-}, $S_2O_3^{2-}$).

Fig. S15 Fluorescence spectral changes of **DAS** in presence of all anions and AcO^- in methanol-water medium at 25 °C.

Fig. S16 Fluorescence spectral changes of **DAS** in presence of all anions and F^- in methanol-water medium at 25 °C.

Fig. S17 Fluorescence spectral changes of **DAS** (25 μM) with F^-, inset shows calibration curve for determination of LOD.

Fig. S18 Decay profiles of **DAS** and **DAS**-F^- adduct (λ_{ex}=375 nm).

Fig. S19 ^{1}H-NMR spectra of **DAS** in d_6-DMSO after addition of 0-2 equivalents of fluoride ion.

Fig. S20 Absorption spectra of **DAS** at different pH levels (3-9).

Fig. S21 Absorption spectra of **DAS** at extreme pH levels.

Fig. S22 Plot of absorbance vs. pH at wavelength 410 and 368 nm.

Fig. S23 The detection of F^- from toothpaste and fluoride free toothpaste by colour change under UV lamp.

Table S1 Coordination bond distances (Å) and angles (°) for complex **DAS**.

Table S2 Comparison table of previous relevant studies with LOD.

Table S3 TCSPC experimental results of **DAS** and **DAS**-F^-.

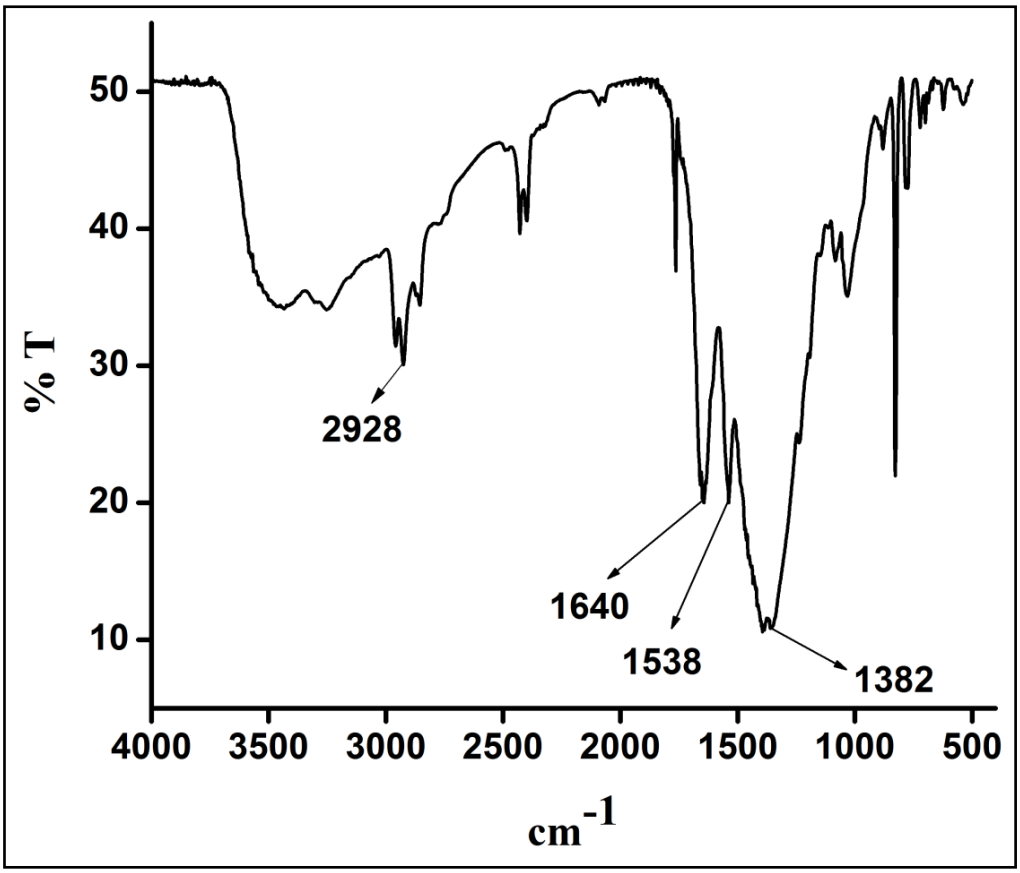

Fig. S1 FT-IR Spectrum of **DAS**.

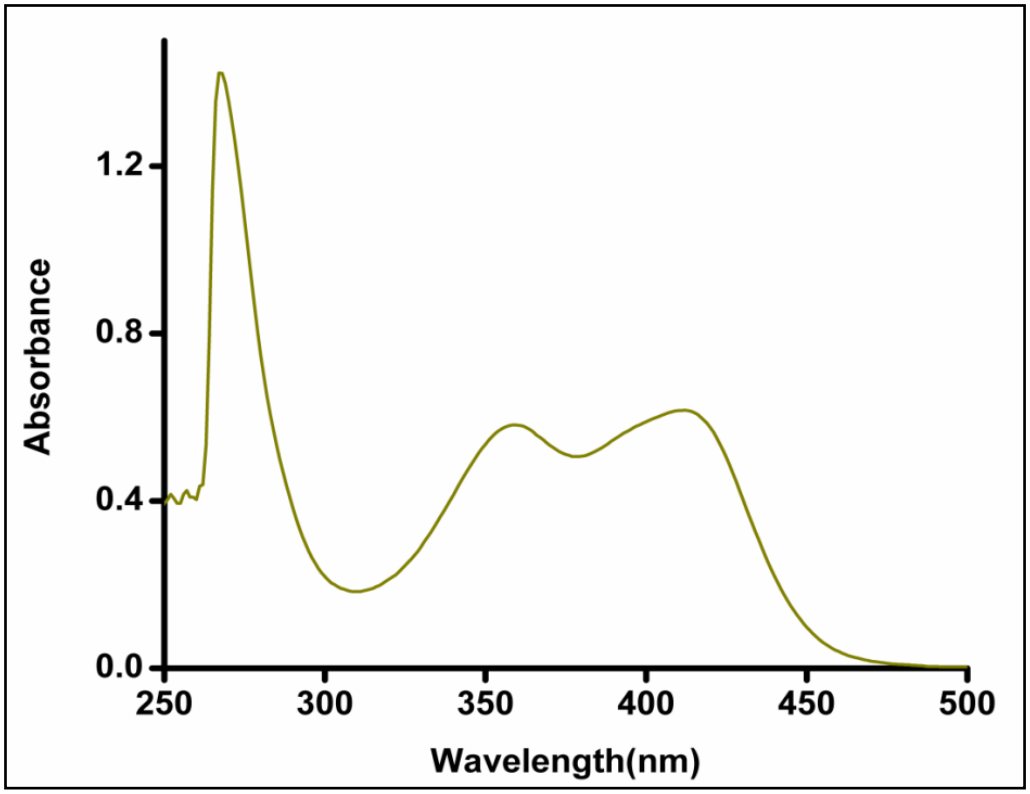

Fig. S2 UV-Vis spectrum of **DAS** in methanol medium at 25 °C.

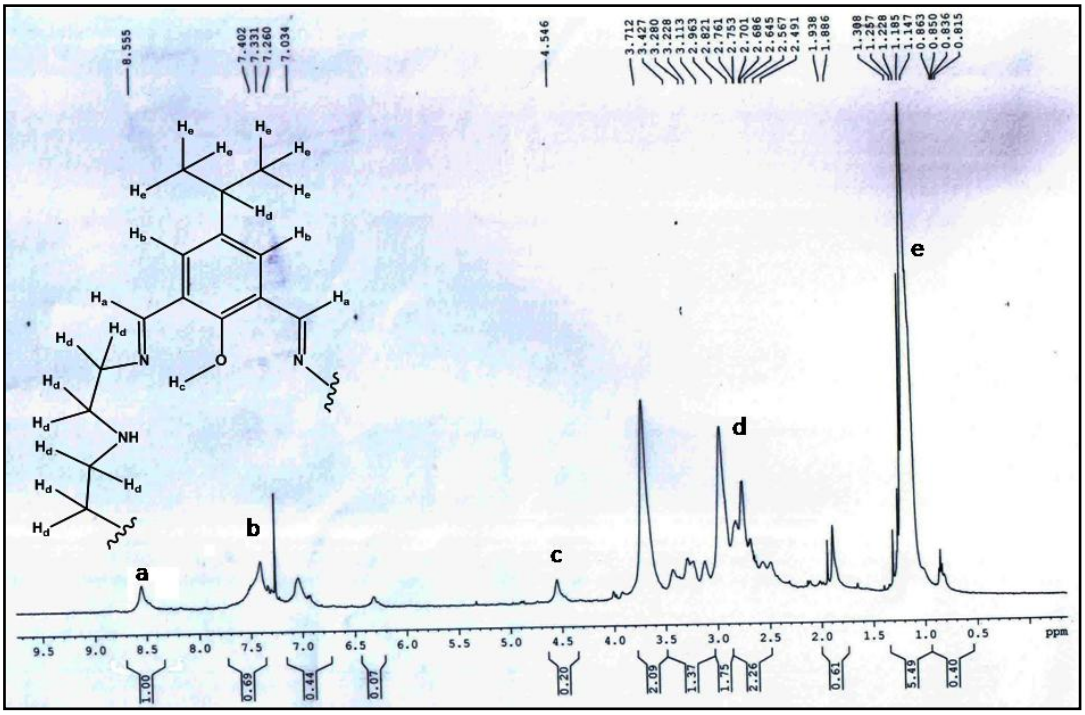

Fig. S3 ^{1}H-NMR spectra of Ligand **(LH_4)** in $CDCl_3$.

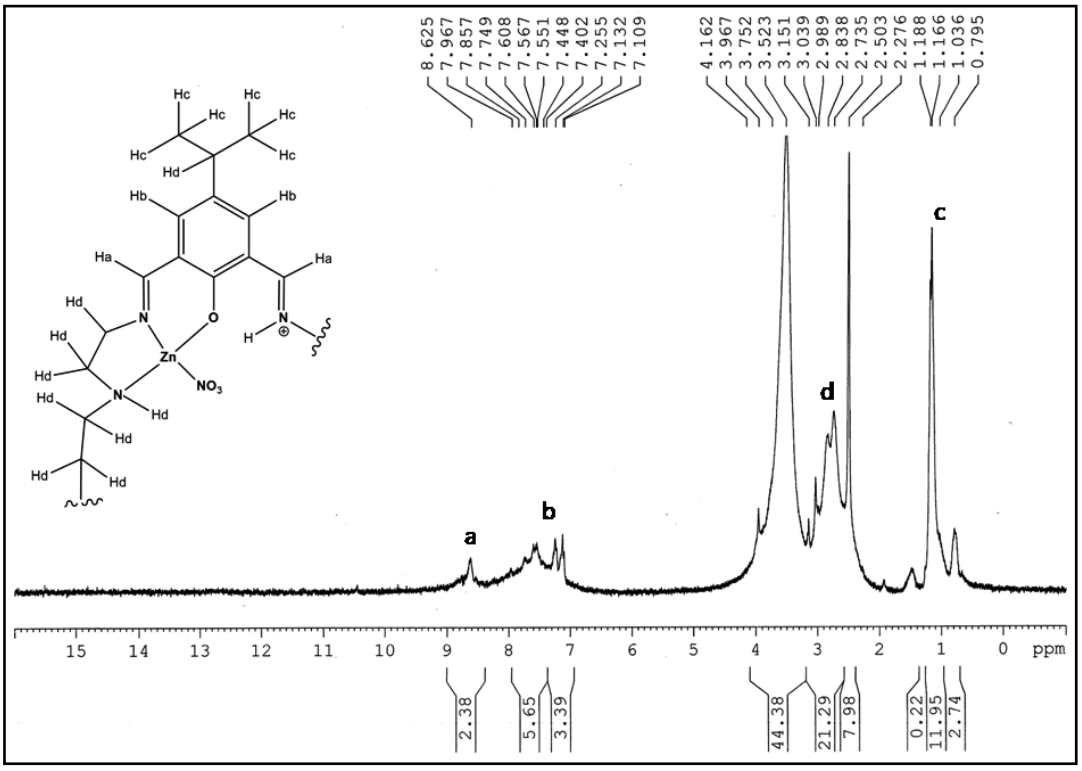

Fig. S4 ^{1}H-NMR spectra of **DAS** in d_6-DMSO.

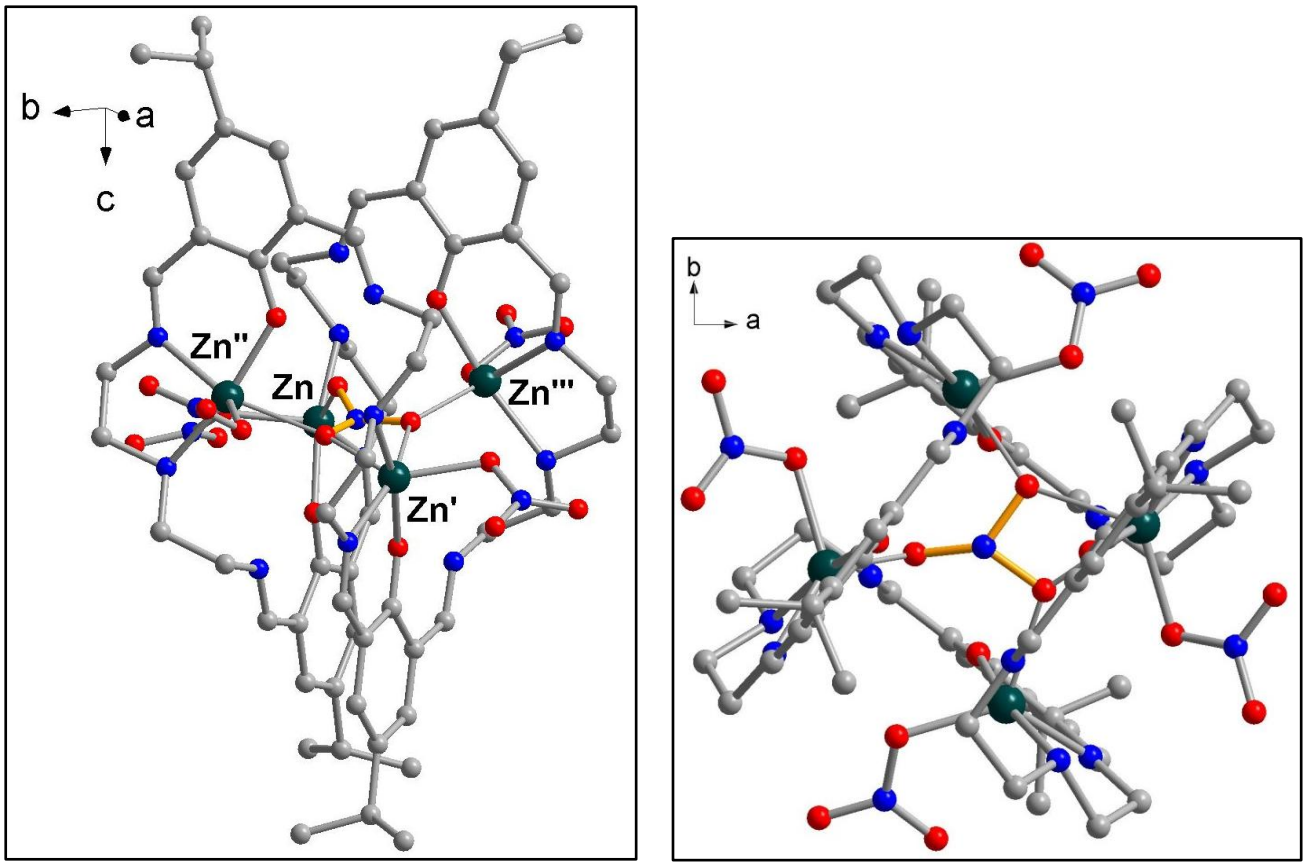

(a) (b)

Fig. S5 (a) The molecular structure of the tetranuclear **DAS** complex and (b) a view down the improper fourfold axis (only one of four disordered orientations of nitrate in the core is shown for clarity).

Table S1 Coordination bond distances (Å) and angles (°) for complex **DAS**

Zn(1)-O(1)	2.003(10)	Zn(1)-O(6)	1.94(3)
Zn(1)-N(1)	2.085(13)	Zn(1)-O(5)	2.23(4)
Zn(1)-N(2)	2.113(12)	Zn(1)-O(5')	2.20(4)
Zn(1)-O(2)	2.063(11)		
O(1)-Zn(1)-N(1)	85.7(5)	N(1)-Zn(1)-O(5')	154.9(7)
O(1)-Zn(1)-N(2)	167.2(4)	N(2)-Zn(1)-O(2)	101.4(5)
O(1)-Zn(1)-O(2)	89.9(5)	N(2)-Zn(1)-O(6)	90.2(11)
O(1)-Zn(1)-O(6)	95.7(10)	N(2)-Zn(1)-O(5)	94.9(8)
O(1)-Zn(1)-O(5)	84.4(8)	N(2)-Zn(1)-O(5')	110.3(10)
O(1)-Zn(1)-O(5')	79.1(10)	O(2)-Zn(1)-O(5)	120.2(9)
N(1)-Zn(1)-N(2)	82.5(5)	O(2)-Zn(1)-O(6)	90.8(14)

N(1)-Zn(1)-O(2)	129.9(5)	O(2)-Zn(1)-O(5')	70.3(8)
N(1)-Zn(1)-O(6)	139.3(14)	O(5)-Zn(1)-O(5')	50.2(11)
N(1)-Zn(1)-O(5)	108.9(9)		

Atom O(5') at y+1/2,-x+3/2,-z+1/2.

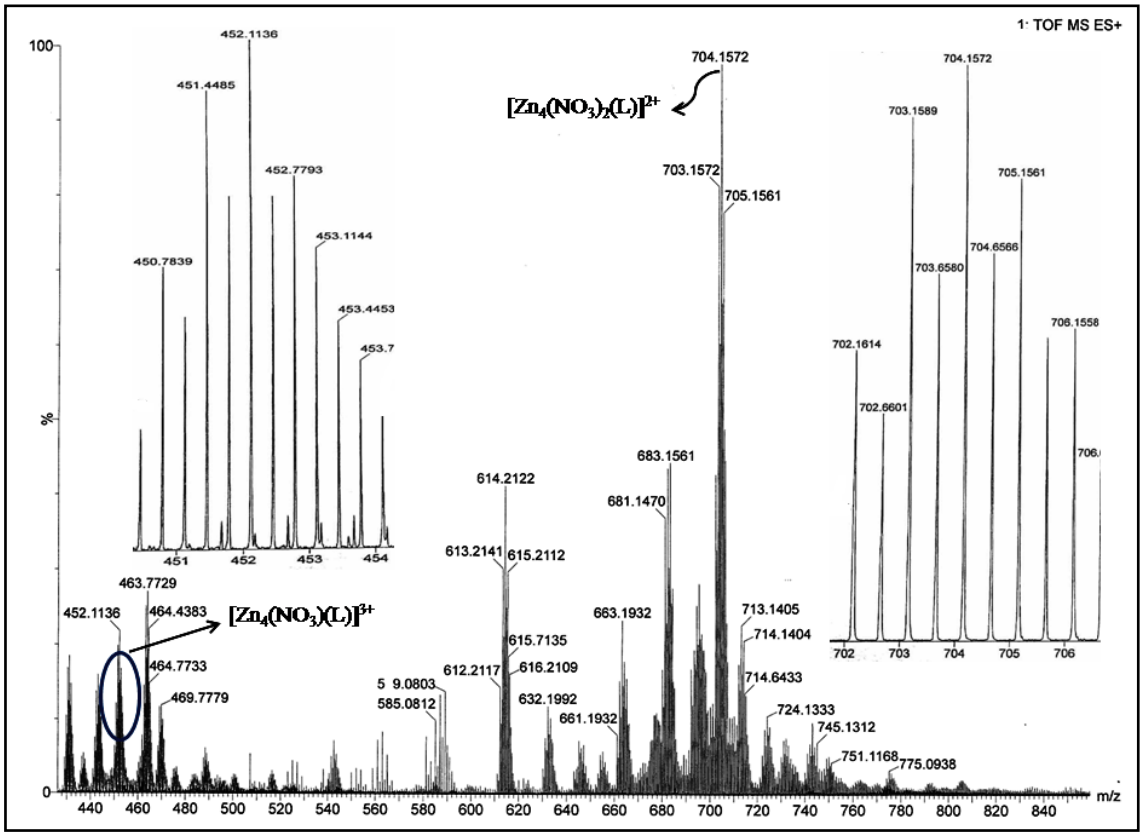

Fig. S6 ESI-MS spectra of **DAS**. The inset clearly shows the differences in spacing for the dipositive and tripositive moiety of **DAS** in solution.

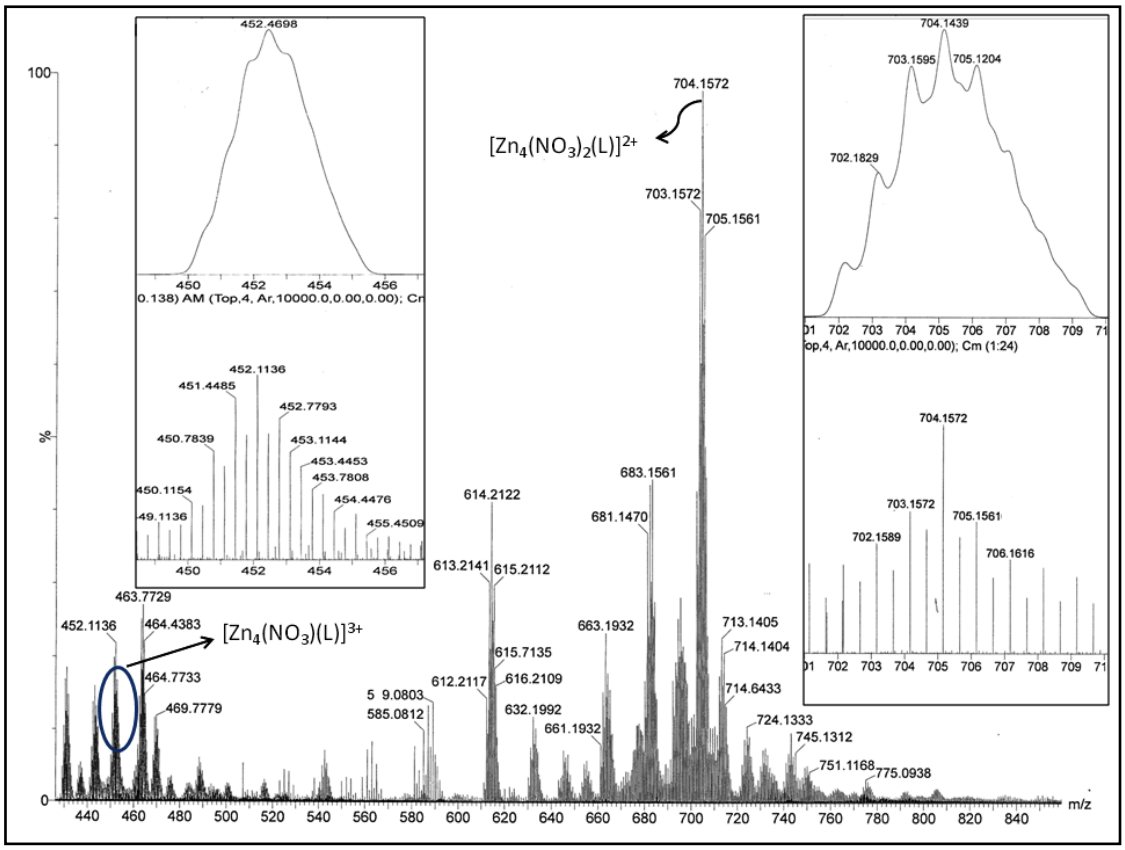

Fig. S7 ESI-MS spectra with theoretical simulation of **DAS**.

(a) (b)

Fig. S8 Color change of **DAS** (75μM) (a) under ambient light, (b) under UV-light upon addition of 10 equivalents of F^-, AcO^- compared to other anions (Cl^-, I^-, S^{2-}, PO_4^{3-}, $S_2O_3^{2-}$).

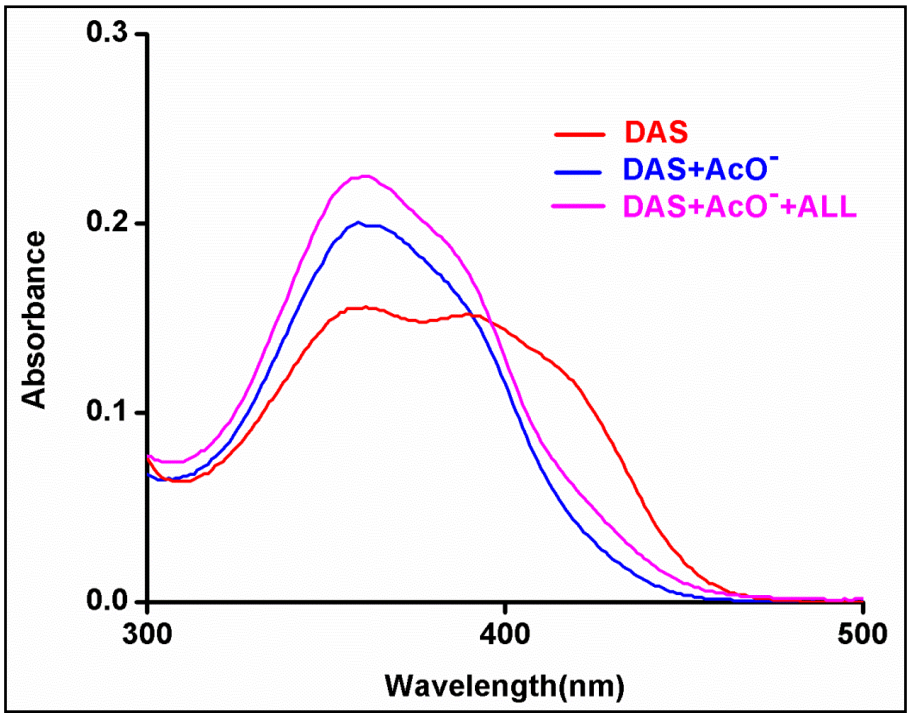

Fig. S9 UV-Vis response of **DAS** in presence of all anions and AcO^- in methanol-water medium at 25 °C.

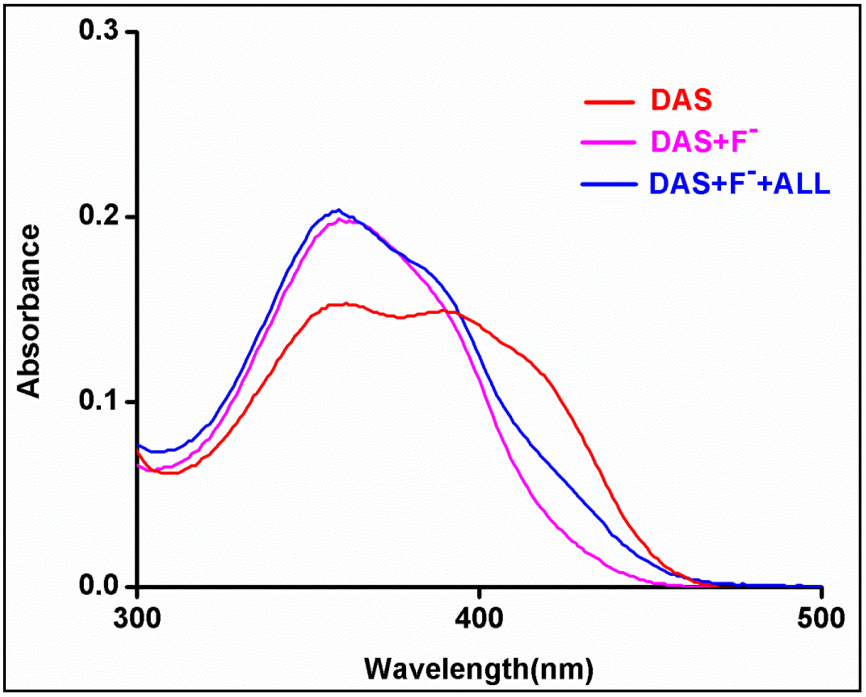

Fig. S10 UV-Vis response of **DAS** in presence of all anions and F^- in methanol-water medium at 25 °C.

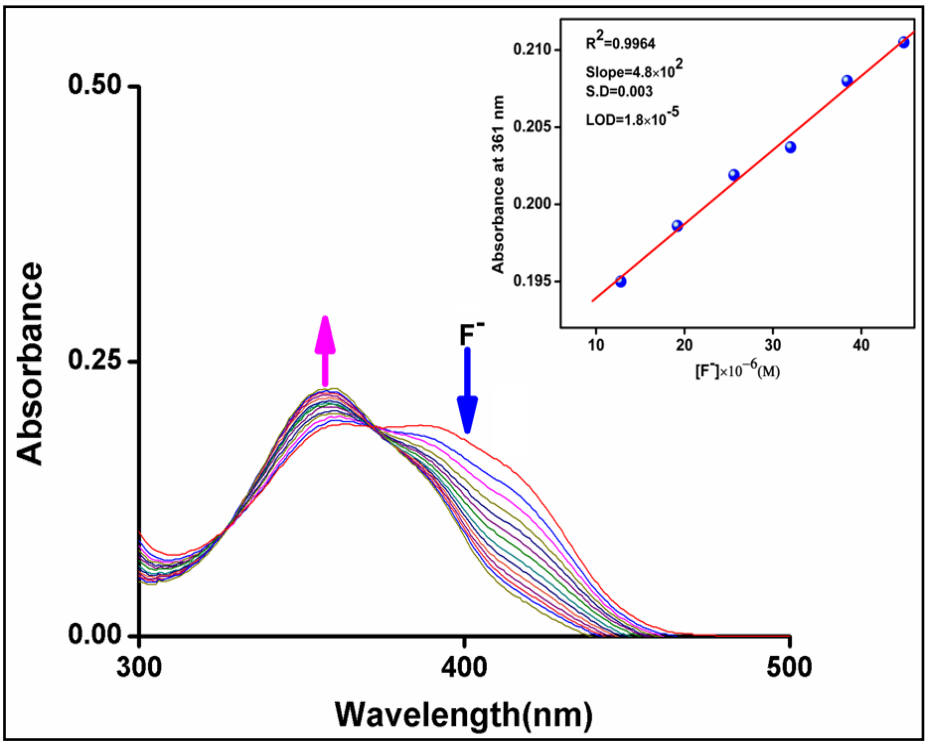

Fig. S11 UV-Vis titration of **DAS** (25 μM) with F^-, inset shows calibration curve for determination of LOD.

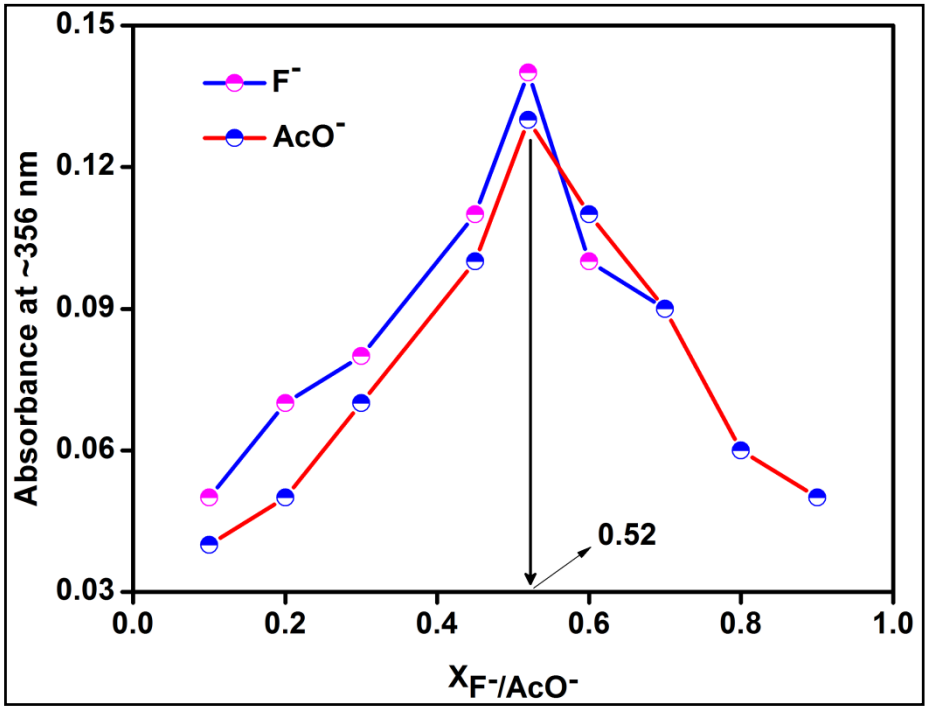

Fig. S12 Job's plot for the determination of **DAS**-F^-/AcO^- (1:1) complex stoichiometry using absorbance values.

Table S2 Comparison table of previous relevant studies with LOD

Serial no	Sensor	Anion	Solvent	LOD	Reference
1	4-nitro-2-((pyrimidin-2-ylamino) methyl) phenol	F^- and OAC^-	Acetonitrile	1.0025×10^{-7}(M) and 0.79×10^{-7}(M)	1
2	**HNHCB** (3-hydroxynaphthalene-2-carboxylic acid (4-cyanobenzylidene)-hydrazide)	F^-	Acetonitrile /water	1.3×10^{-6}(M)	2
3	**(ADAMN)** 2-((anthracen-10-yl)methyleneamino)-3-aminomaleonitrile	F^-	Acetonitrile	5.0×10^{-6} (M)	3
4	Vitamin B_6 Schiff base analog	F^-	Dimethylsulfoxide (DMSO)	7.39×10^{-8} (M)	4
5	Acridine-based thiosemicarbazone	F^-	Dimethylsulfoxide (DMSO)	9.08×10^{-5}(M)	5
6	6H-indolo[2,3-b]quinoline	F^-	Dimethylsulfoxide (DMSO)	0.2×10^{-6}(M)	6
7	4-nitro-benzenesulfonic acid 4-methyl-2-oxo-2H-chromen-7-yl ester	F^-	Acetonitrile	77.82×10^{-9}(M)	7
8	Vitamin B6 cofactors like pyridoxal (PL)	OAC^-	DMSO/water	7.37×10^{-6} (M)	8
9	Vitamin B6 cofactors like pyridoxal-5-phosphate (PLP)	OAC^-	DMSO/water	2.29×10^{-5}(M)	8
10	4-(thiazol-2-yldiazenyl)phenol	OAC^-	DMSO/water	83.0×10^{-9}(M)	9
11	2-((4-hydroxyphenyl) diazenyl)-5-nitrophenol	OAC^-	DMSO/water	83.0×10^{-9}(M)	9
12	DAS	F^-	Methanol /water	0.18×10^{-6}(M)	**Our work**
13	DAS	OAC^-	Methanol /water	1.98×10^{-6}(M)	**Our work**

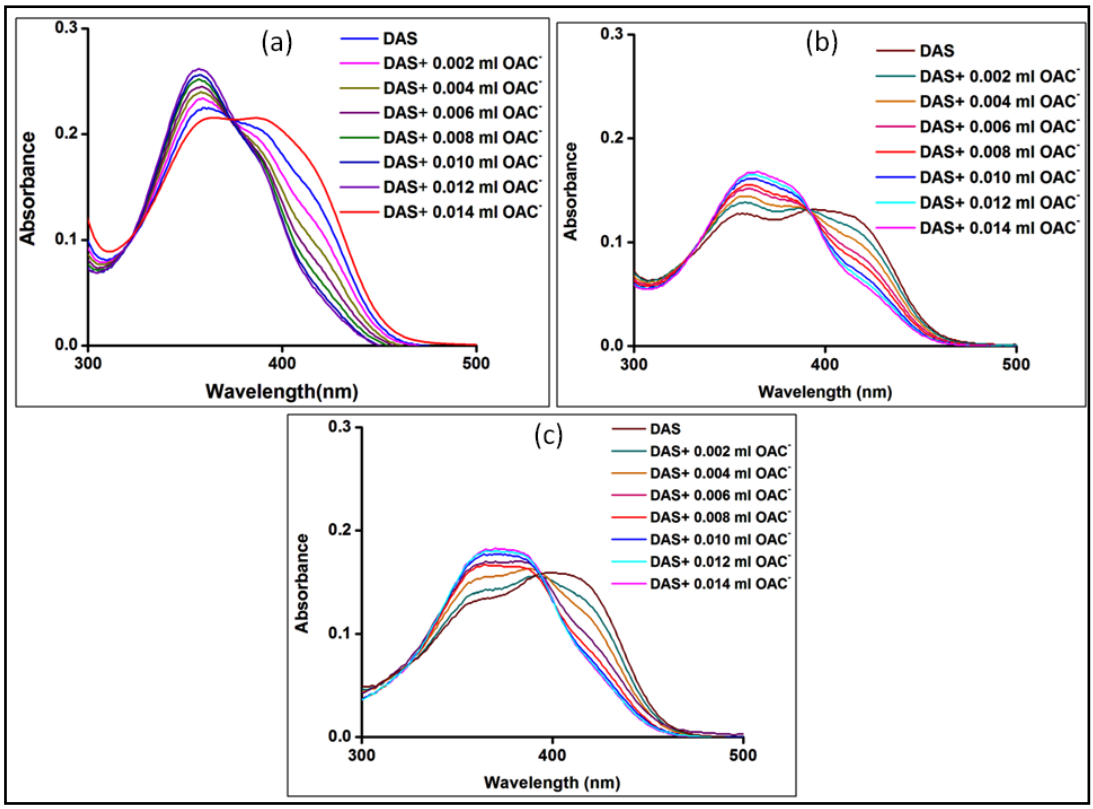

Fig. S13 UV-Vis titration of **DAS** (25 μM) with AcO^- in (a) methanol (b) acetonitrile (c) acetonitrile-methanol (2:1) medium at 25 °C.

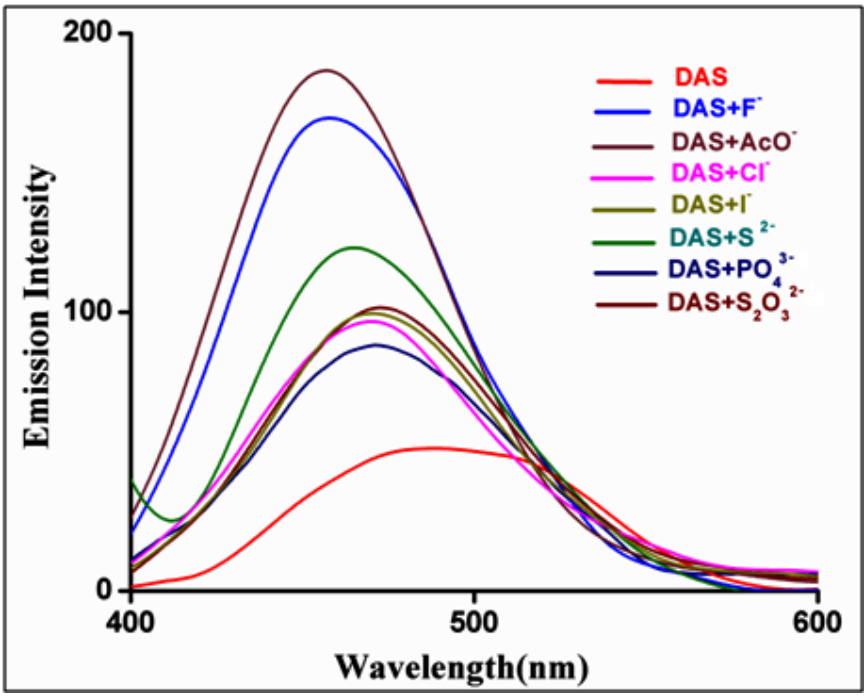

Fig. S14 Fluorescence spectrum of **DAS** (25 μM) in presence of all anions (F^-, AcO^-, Cl^-, I^-, S^{2-}, PO_4^{3-}, $S_2O_3^{2-}$).

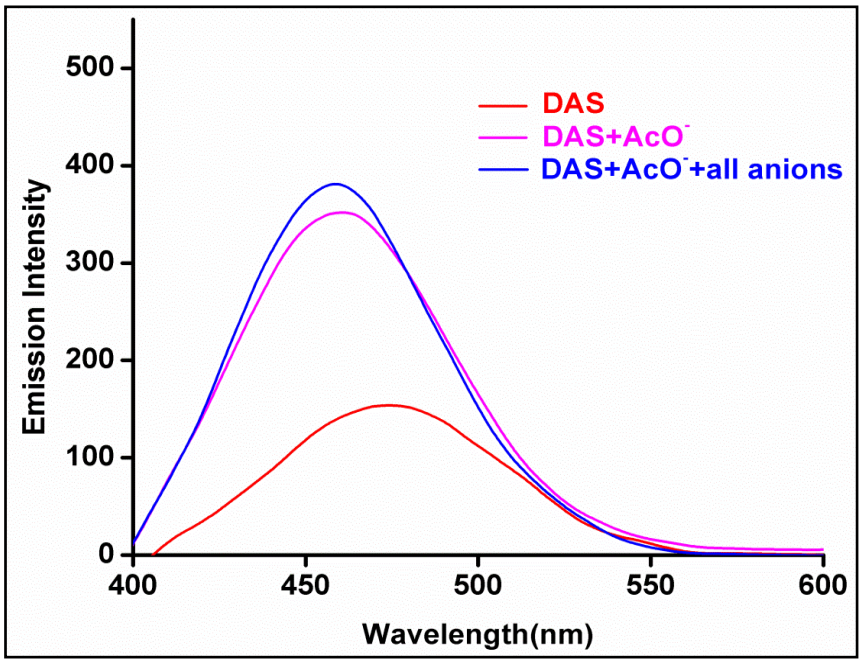

Fig. S15 Fluorescence spectral changes of **DAS** in presence of all anions and AcO^- in methanol-water medium at 25 °C.

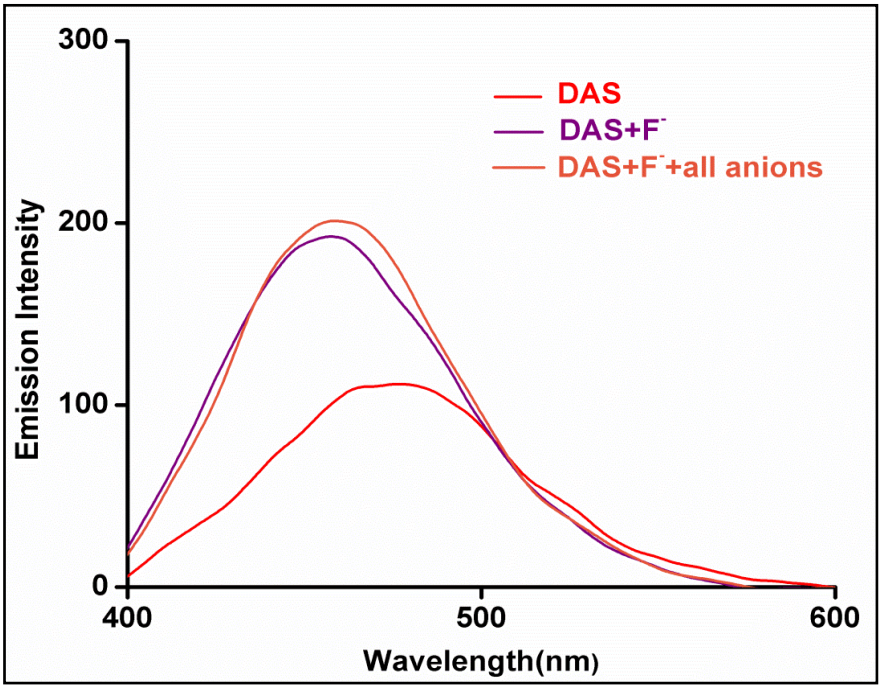

Fig. S16 Fluorescence spectral changes of **DAS** in presence of all anions and F^- in methanol-water medium at 25 °C.

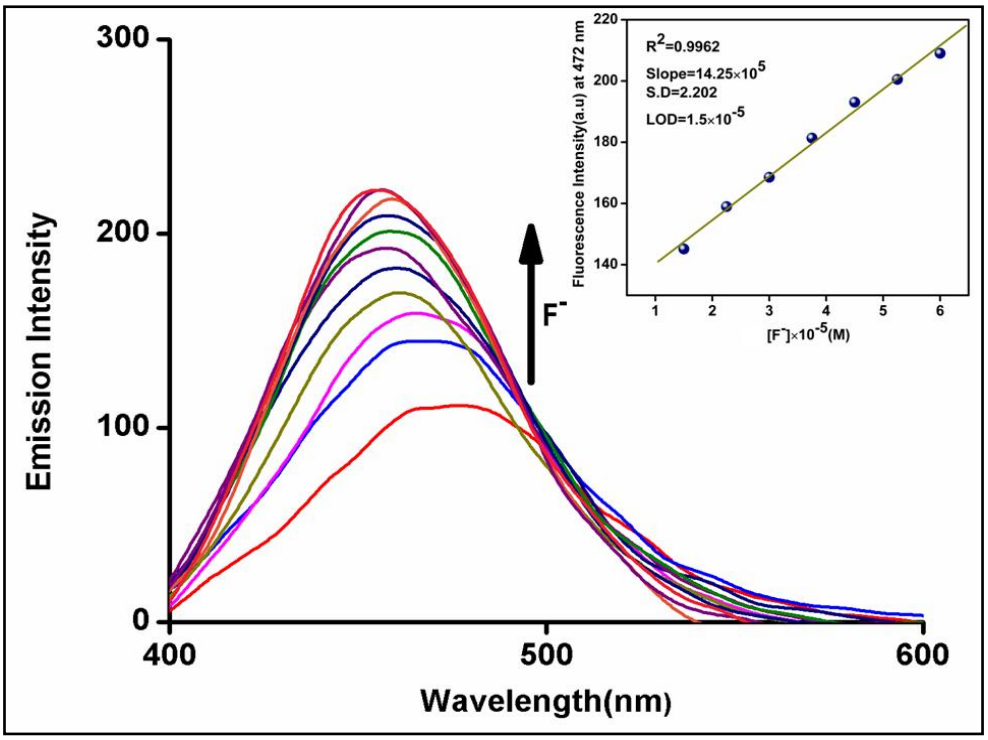

Fig. S17 Fluorescence spectral changes of **DAS** (25 μM) with F^-, inset shows calibration curve for determination of LOD.

Table S3 TCSPC experimental results of **DAS** and **DAS**-F^-

λ_{mon}	Species	τ_1(ns)	τ_2(ns)	α_1	α_2	χ^2	τ_{av}(ns)
450	**DAS**	0.76 ns	4.61 ns	0.94	0.06	1.19	0.97
475	**DAS**	0.81 ns	4.83 ns	0.93	0.07	1.15	1.11
450	**DAS**-F^-	0.73 ns	4.49 ns	0.95	0.05	1.15	0.92
475	**DAS**-F^-	0.79 ns	4.93 ns	0.92	0.08	1.05	1.14

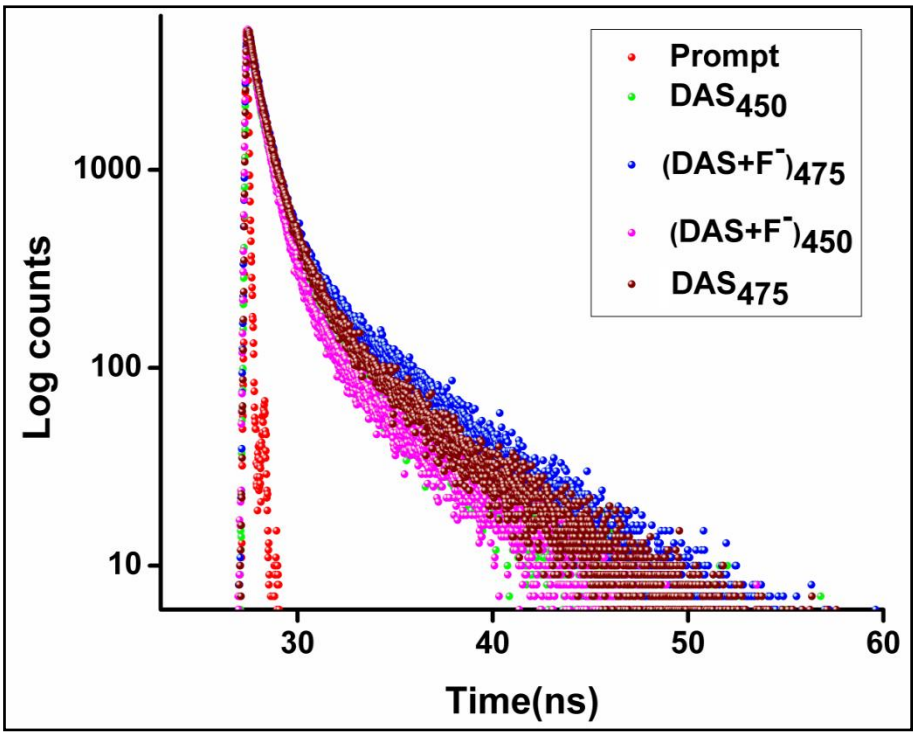

Fig. S18 Decay profiles of **DAS** and **DAS**-F^- adduct (λ_{ex}=375 nm).

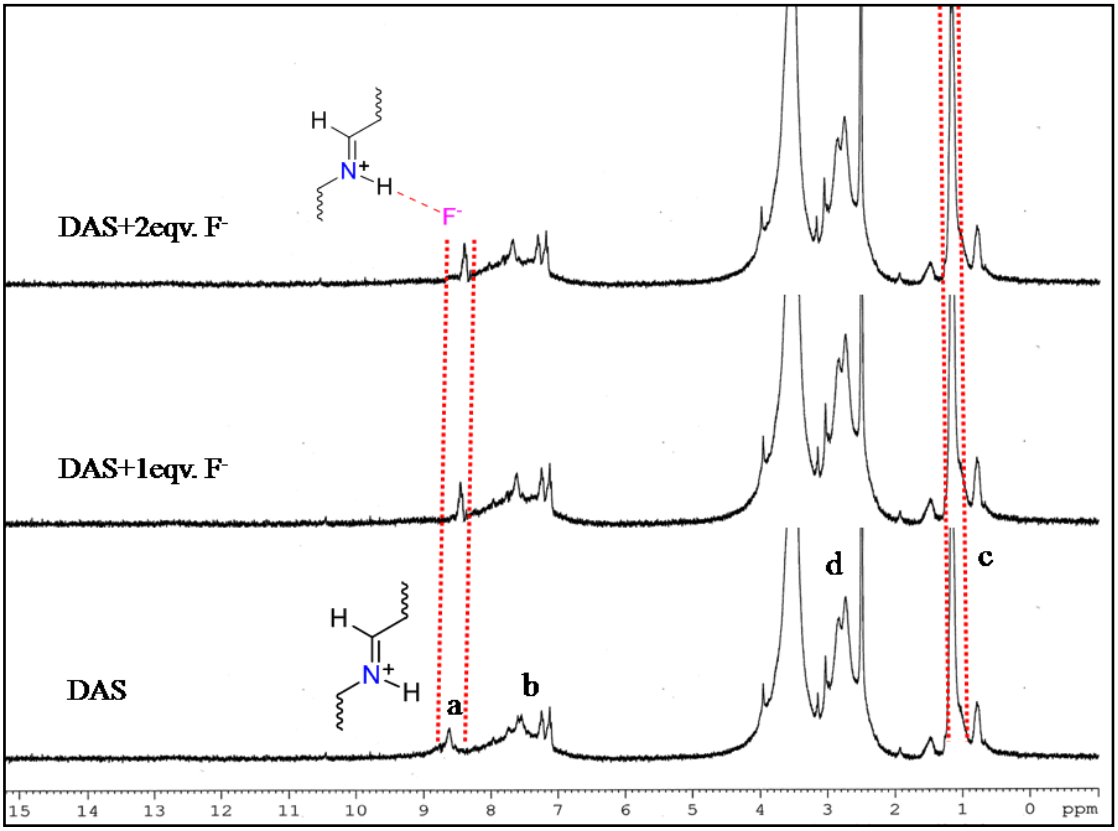

Fig. S19 ^{1}H-NMR spectra of **DAS** in d_6-DMSO after addition of 0-2 equivalents of fluoride ion.

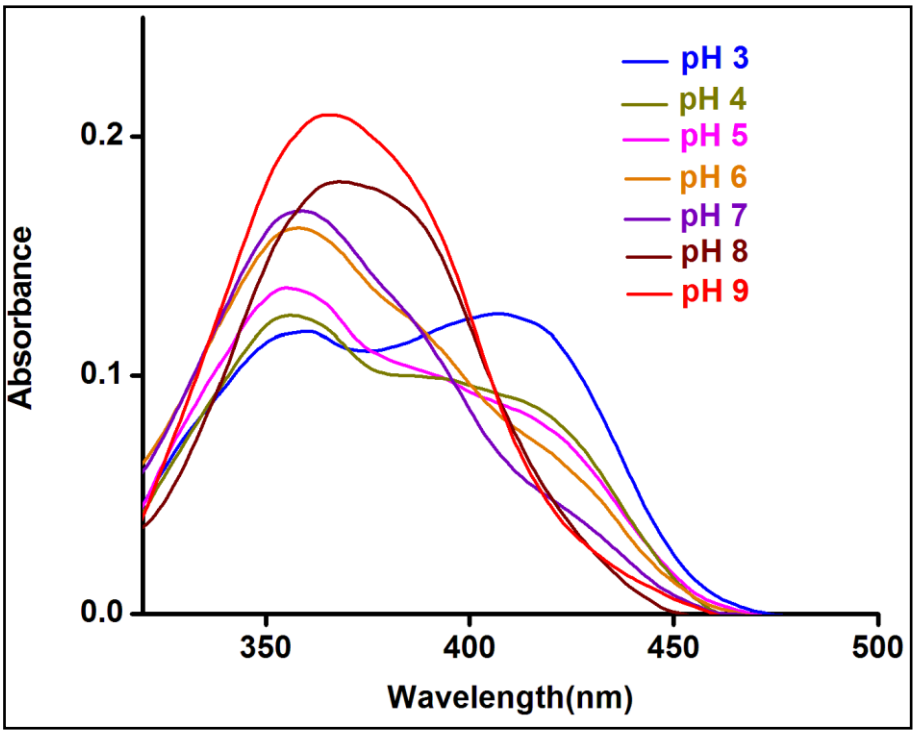

Fig. S20 Absorption spectra of **DAS** at different pH levels (3-9).

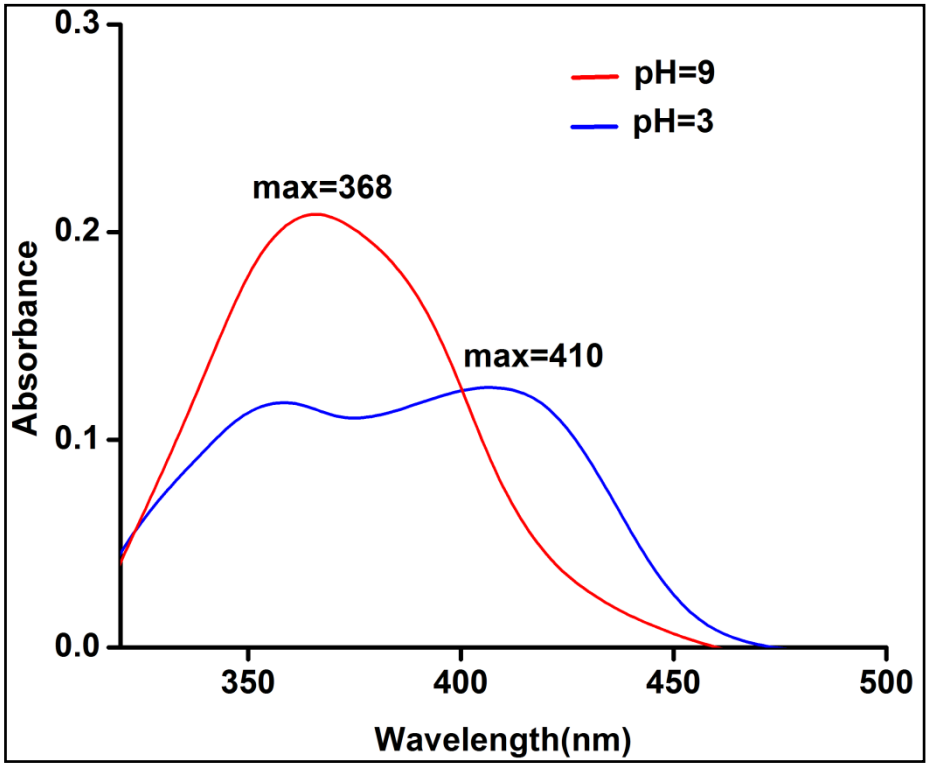

Fig. S21 Absorption spectra of **DAS** at extreme pH levels.

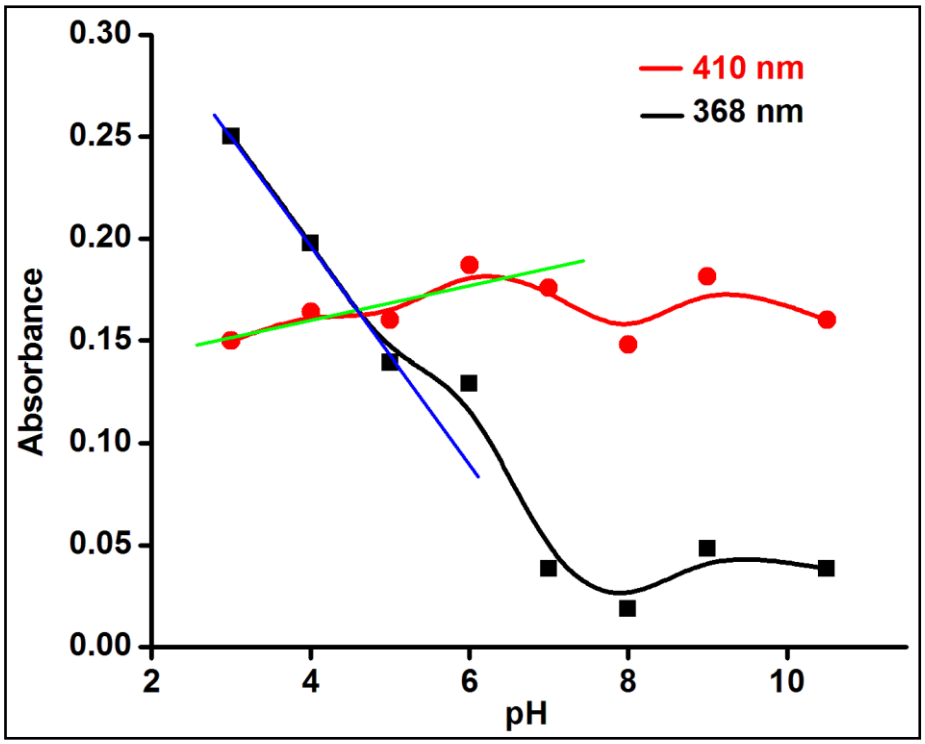

Fig. S22 Plot of absorbance vs. pH at wavelength 410 and 368 nm.

Calculation of pk_a

Fig. S21 represents the spectra of **DAS** with extreme pH levels (pH = 3 and pH = 9 in this case) and determine the wavelengths of maximum absorbance, at pH = 3 exhibited a peak at 410 nm, the peak at pH = 9 occurred at 368 nm. The plot of the absorbance vs. pH at these wavelengths is presented in Fig. S22. And the pKa was obtained by determining the pH of the point of intersection of the two linear curves as shown in Fig. S22. To determine this point, the linear equations of the two points closest to the crossing at each curve.

$$-0.05833x+0.4311= -0.004x+.018$$

$$x = 0.2511/0.05433$$

$$\text{pKa}= 4.62$$

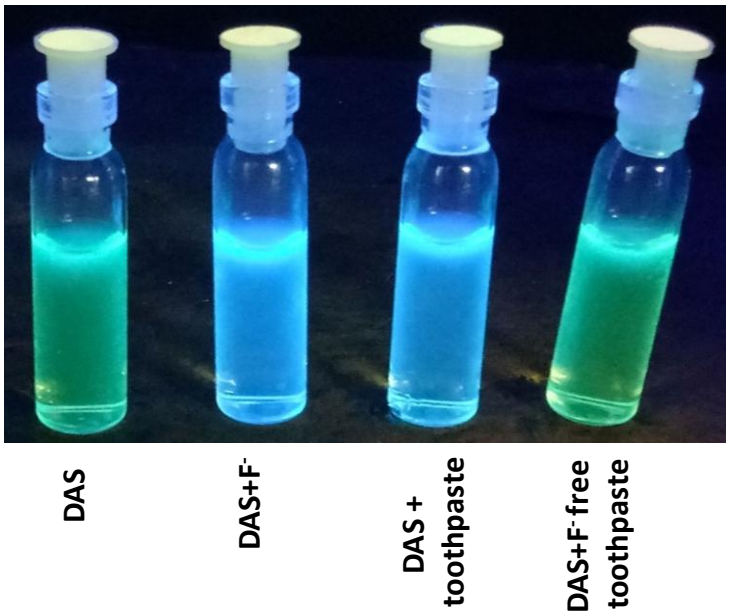

Fig. S23 The detection of F^- from toothpaste and fluoride free toothpaste by colour change under UV lamp.

References

1 A. Bhattacharyya, S. Ghosh, S. C. Makhal, N. Guchhait, *Spectrochimica Acta Part A: Molecular and Biomolecular Spectroscopy.* 2017, **179**, 242-249.

2 S. Ghosh, A. Ganguly, A. Bhattacharyya, M. A. Alam, N. Guchhait, *RSC Adv.* 2016, **6**, 67693-67700.

3 A. Bhattacharyya, S. C. Makhal, A. Ganguly, N. Guchhait, *Chemical Physics Letters.* 2018, **696**, 106-111.

4 D. Sharma, S. K. Sahoo, S. Chaudhary, R. K. Berac, J. F. Calland, *Analyst*. 2013, **138**, 3646-3650.

5 I. O. Isaac, I. Munir, M. al-Rashida, S. A. Ali, Z. Shafiq, M. Islam, R. Ludwig, K. Ayub, K. M. Khan, A. Hameed, *R Soc Open Sci*. 2018, **5**, 180646.

6 R. Pegu, G. Pandit, A. K. Guha, S. K. Das, S. Pratihar, *Spectrochimica Acta Part A: Molecular and Biomolecular Spectroscopy*. 2019, **211**, 246-253.

7 X. Wang, Y. Zhou, C. Xu, H. Song, X. Pang, X. Liu, *Spectrochimica Acta Part A: Molecular and Biomolecular Spectroscopy*. 2019, **211**, 125-131.

8 D. Sharma, A. Kuba, R. Thomas, S. K. A. Kumar, A. Kuwar, H.-J. Choi, S. K. Sahoo, *Spectrochimica Acta Part A: Molecular and Biomolecular Spectroscopy*. 2016, **157**, 110-115.

9 D. Singhal, N. Gupta, A. K. Singh, *Front. Microbiol*. 2019.